# Secondary Atomization of Electrostatically Charged Drops

D. R. Guildenbecher* and P. E. Sojka†
Maurice J. Zucrow Laboratories
School of Mechanical Engineering
Purdue University
West Lafayette, IN 47907 USA

**Abstract**

An investigation was conducted into the secondary atomization of charged drops. It began by deriving a non-dimensional charge number, *Q*, which compares the disruptive electrostatic stresses to the consolidating surface tension stresses. A non-dimensional conductivity number, *K*, was also proposed to compare the rate of charge movement to other characteristic times. Experimental results are presented which cover the range of *Q* and *K* expected in practice. They reveal that charge has a minimal effect on both breakup morphology and breakup time. Rather aerodynamic forces dominate the process. Finally, an analysis of the charge distribution on a deformed drop is presented to explain the small differences observed in results from conductive and non-conductive drops.

## Introduction

Secondary atomization has been extensively studied for the case of *uncharged* Newtonian liquids [1-4]. Only the most relevant findings are summarized here. Interested readers may refer to [4] for a complete discussion.

For *uncharged* drops, fragmentation proceeds in a manner which is dependent on the level of aerodynamic forces. This dependence is illustrated by the breakup morphology shown in Figure 1, where increases from left to right and aerodynamic forces increase from top to bottom. Each row illustrates a different breakup mode.

Experimentalists [1-4] have shown that the breakup morphology and breakup times are a function of Weber number, *We*, and are independent of other parameters, except for highly viscous liquids (not considered here):

$$We = \rho_a U_0^2 d_0 / \sigma \tag{1}$$

Here $\rho_a$ is the density of the ambient fluid, $U_0$ is the initial relative velocity between the drop and the ambient, $d_0$ is the initial spherical diameter, and $\sigma$ is the surface tension. Time is made non-dimensional as suggested by [5]:

$$T = tU_0 \rho_a^{0.5} / \rho_d^{0.5} d_0 \tag{2}$$

Here *T* is the non-dimensional time, *t* is the dimensional time, and $\rho_d$ is the density of the drop.

In an electrospray, a voltage is applied to enhance atomization. This leads to the formation of drops with non-zero charge. If exposed to a high-speed gas stream, these charged drops may undergo secondary atomization. Despite many practical applications, no experimental investigation of charged secondary atomization is known to exist.

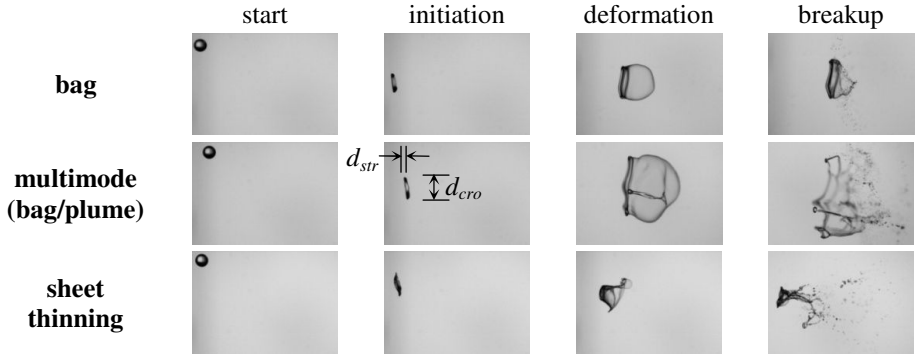


**Figure 1.** Uncharged Newtonian breakup morphology

* This material is based upon work supported under a National Science Foundation Graduate Research Fellowship
† Corresponding author

For a conductive drop, electrostatic charge migrates to its surface. At the surface, electrostatic repulsion creates a normal stress that is proportional to the square of the surface charge density [6]:

$$\Delta p_{e^-} = \gamma^2 / 2\varepsilon_0 \tag{3}$$

Here $\Delta p_{e^-}$ is the normal stress due to surface charge, $\gamma$ is the surface charge density, and $\varepsilon_0$ is the permittivity of the surrounding fluid. The stress acts in a direction that tends to draw the liquid into the surroundings. Countering this is the normal stress due to surface tension, given by $\Delta p_\sigma = 4\sigma / d_0$.

Assuming an initially spherical drop with a uniform surface charge density of $\gamma_0 = q/\pi d_0^2$, a stationary drop becomes unstable when $\Delta p_{e^-} = \Delta p_\sigma$. At this point $q = q_{Ra}$, where $q_{Ra}$ is the Rayleigh charge limit [7]:

$$q_{Ra} = \sqrt{8\pi^2 \sigma \varepsilon_0 d_0^3} \tag{4}$$

In this investigation we consider the combined effects of charge and aerodynamic forces. Therefore, $q < q_{Ra}$.

An initial attempt at modeling this situation was given by [8]. After assuming charge results in uniform reduction in the "effective surface tension" an electrostatic Weber number, $We_{e^-}$, was derived:

$$We_{e^-} = \rho_a U_0^2 d_0 \Big/ \left(\sigma - q^2 / 8\pi^2 \varepsilon_0 d_0^3\right) \tag{5}$$

It was theorized that the traditional $We$ can be replaced by $We_{e^-}$. Unfortunately, the assumption of a uniform reduction in surface tension is only true initially (a spherical drop with constant charge density). Eq. (3) reveals that unlike surface tension, electrostatic forces are not proportional to surface curvature. Therefore, a non-uniform reduction in the "effective surface tension" will occur, and the use of $We_{e^-}$ is unlikely to be valid for all cases.

Alternatively we propose a non-dimensional charge number, $Q$, which compares the electrostatic stress to the surface tension stress for the initially spherical drop:

$$Q = q^2 / 8\pi^2 \varepsilon_0 \sigma d_0^3 \tag{6}$$

Note that $Q = (q/q_{Ra})^2$ such that $Q \rightarrow 1$ when $q = q_{Ra}$ and the drop is unstable. Also, $Q = 0$ when the drop is uncharged.

Previous investigations of electrostatic *primary* atomization [9] have shown that breakup is not only a function of charge level but also depends on the rate of charge movement. It is therefore reasonable to assume that a similar dependence exists for secondary atomization.

All fluids possess some level of resistivity resulting in a finite rate of charge movement. This can be characterized by the charge relaxation time:

$$\tau = \kappa \varepsilon_0 / k \tag{7}$$

Here $\kappa$ is the dielectric constant and $k$ is the electrical conductivity. When a non-dimensional group is formed using Eq. (7) and the time scale factor given in Eq. (2), the result is referred to as the conductivity number, $K$:

$$K = \kappa \varepsilon_0 \rho_d^{0.5} U_0 \Big/ \rho_a^{0.5} d_0 k \tag{8}$$

Note that when $K << T_{tot}$, where $T_{tot}$ is the non-dimensional total breakup time, the rate of charge movement is much faster than the rate of drop deformation. Therefore, the charge will adjust itself to achieve a distribution which minimizes electrostatic stresses. Similarly with $K >> T_{tot}$ the charge positions are essentially frozen during the breakup process. It is therefore reasonable to suppose that different breakup modes may be observed for highly conductive and non-conductive liquids.

The study described here was performed to investigate the effect of aerodynamic drag on electrically charged Newtonian drops. The breakup morphology, initiation time, and total breakup time are reported. Wide ranges of charge and conductivity numbers are considered which encompass ranges expected in practical applications.

It is important to note that initial results of this investigation were presented previously [10, 11]. Following them our experimental setup was improved. Any differences between the results and conclusions given here and those in the previous papers are addressed.

**Table 1.** Liquid physical properties

| | Water + 0.4% NaCl (v/v) | Ethyl Alcohol | Hexane + 5% Ethyl Alcohol (v/v) | |
|---|---|---|---|---|
| Density, $\rho_d$ [kg/m$^3$] | 995 ± 9 | 778 ± 7 | 656 ± 3 | |
| Surface tension, $\sigma$, [dynes/cm] | 73.3 ± 0.1 | 24.4 ± 0.1 | 20.2 ± 0.1 | [a] [12] |
| Electrical conductivity, $k$, [S/m] | 0.15 ± 0.01 | 7.8 x $10^{-6}$ ± 1 x $10^{-7}$ | 5.0 x $10^{-11}$ [c] | [b] [13] |
| Dielectric constant, $\kappa$ | 77.7 [a] | 24.6 [b] | 2.0 [c] | [c] [14] |

**Materials and Methods**

Three liquids were selected, with their relevant physical properties given in Table 1. Unless otherwise noted all material properties were measured in the laboratory. Uncertainties were calculated using the method of [15].

Charged drops were produced using the dripping mode described in [9]. Before entering the disruptive air flow field, the charge on each drop was measured using the inductive device show in Figure 2 and based on [16]. It consists of a stainless steel charge pickup tube with induced voltage measured using an operational amplifier specified for an ultralow input bias current (Analog Devices AD549). The op-amp path to ground was achieved with a 10 MΩ resistor.

When a drop enters the tube, an equal and opposite charge is induced. As shown in [16], if the response time of the measurement system is significantly shorter than the length of time it takes the drop to pass through the tube, integration of the current yields the charge on the drop. The inverse process occurs when the drop leaves the tube. The net result is the voltage response shown in Figure 3.

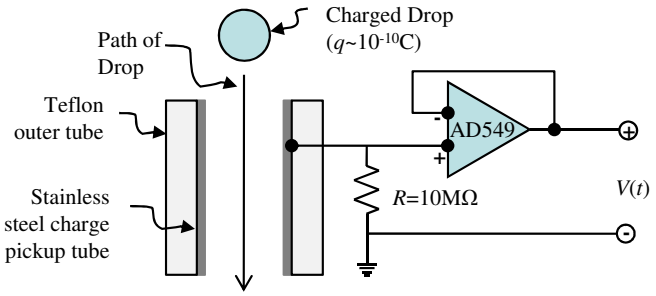


**Figure 2.** Charge measurement device

The charge that passes through the resistor can be found using Ohm's law and integrating the current [16]:

$$q(t) = \int_0^t \frac{V(t)}{R}\,dt \tag{9}$$

Here $V(t)$ is the voltage, $R$ is the resistance, and $q(t)$ is the charge as a function of time. The graph on the right in Figure 3 was calculated using Eq. (9). Note that integration effectively eliminates noise in the signal. Also, two measurements of the charge are possible: one as the drop enters the tube and the total charge goes from zero to its maximum value, and one as the drop leaves the tube and the total charge goes from its maximum value to its final value. By comparing these measurements and assuming other sources of error are minimal, an estimation of the uncertainty in the charge measurement is possible. This is an improvement over the method of [16] which may not effectively eliminate noise and does not provide an estimate of uncertainty.

Drops were directed downward toward a horizontal air jet created using a nozzle, a process similar to the method of [17]. In [4] we define a criterion, which when met ensures that results obtained from air jet experiments are equivalent to those from shock tube experiments. This allows our results to be compared to most correlations available in the literature. Care was taken to ensure that this criterion was met for all results given here.

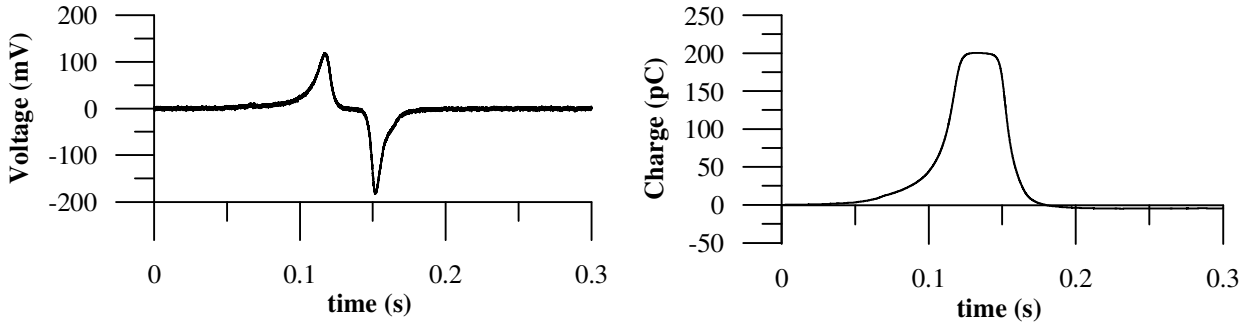


**Figure 3.** Voltage response of the detector and the charge determined by Eq. (9)

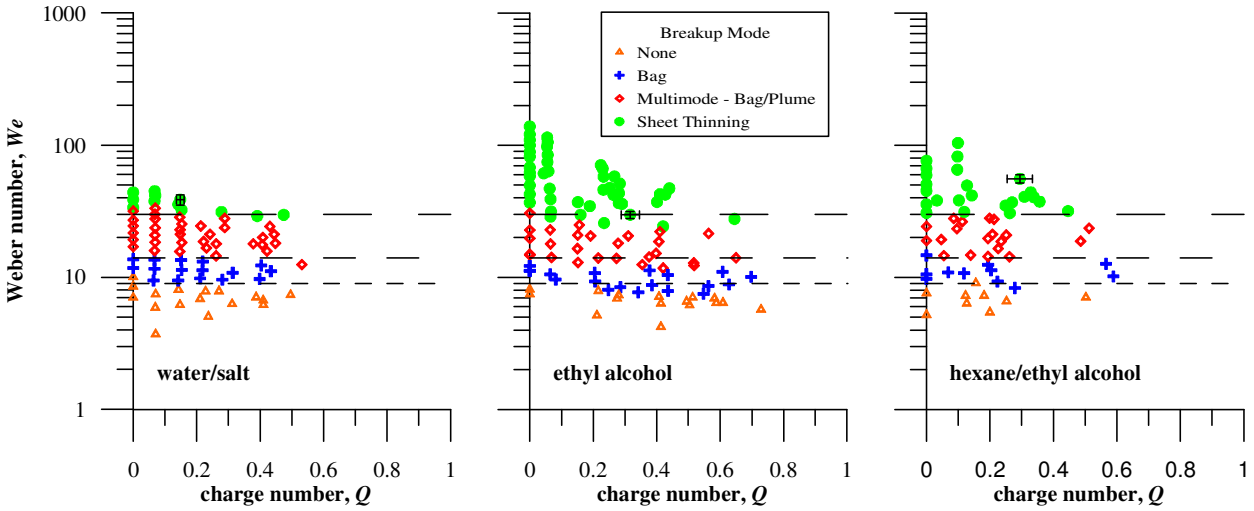


**Figure 4.** Charged Newtonian breakup morphology (typical uncertainty bars shown)

## Results

Approximately 260 movies of drop breakup were recorded covering a wide range of operating conditions ($0<We<140$, $0<Q<0.7$, $1\text{x}10^{-7}<K<200$). In each case the breakup mode was determined by comparison with Figure 1. Despite the presence of charge, no new breakup modes were observed.

Figure 4 shows the breakup mode as a function of $We$ and $Q$ for all three liquids. Different symbols are given for each mode. Uncertainty bars are included.

The data demonstrate that the transition between breakup modes takes place at constant values of $We$, independent of the level of charge. These transition $We$ are shown as horizontal dashed lines. Bag breakup begins at $We\approx9$, multimode at $We\approx14$, and sheet thinning at $We\approx30$. One notable exception is the transition to bag for moderate to low conductivity liquids (ethyl alcohol and hexane/ethyl alcohol) for which $K > 0.01$. In these cases the stability appears to decrease slightly with $Q$.

Results for initiation time, $T_{ini}$, are shown in Figure 5. $T_{ini}$ is defined as the interval between when the drop enters the jet boundary layer ($U\approx0.01U_0$) and when the deformed periphery of the drop is at the same axial plane as the un-deformed trailing edge (second column in Figure 1). This definition, although slightly different from the literature [1, 2], is advantageous in that it does not require separate $T_{ini}$ definitions for each mode. Also, it is relatively straightforward to determine from the movies, so uncertainty due to human judgment is reduced. Finally, correlations taken from previous investigations [1, 2] involving *uncharged* drops are also shown.

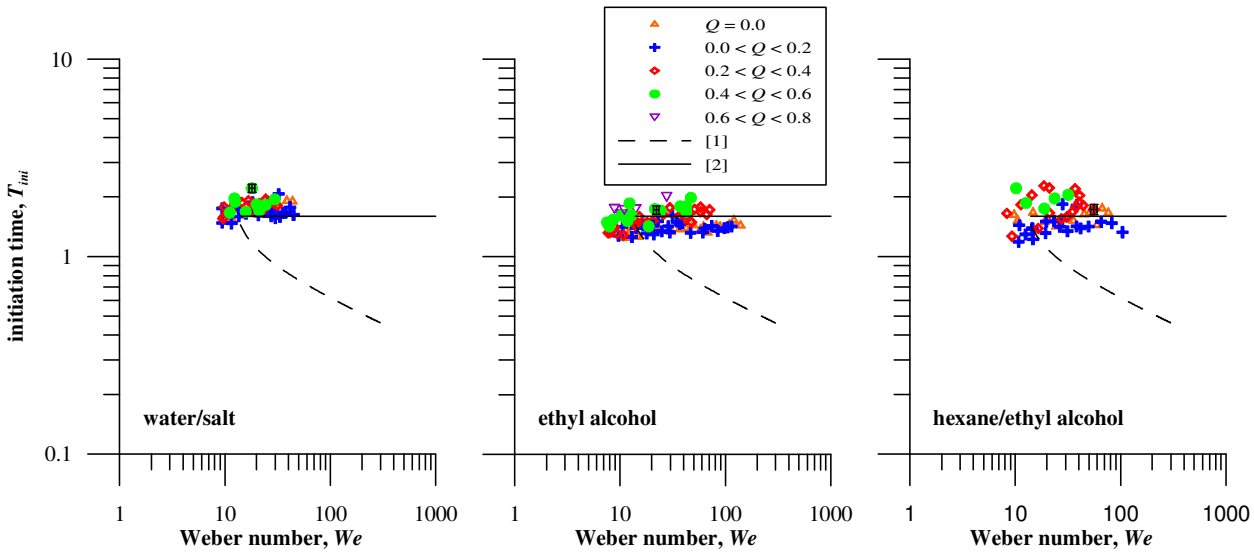


**Figure 5.** Charged Newtonian initiation time, $T_{ini}$ (typical uncertainty bars shown)

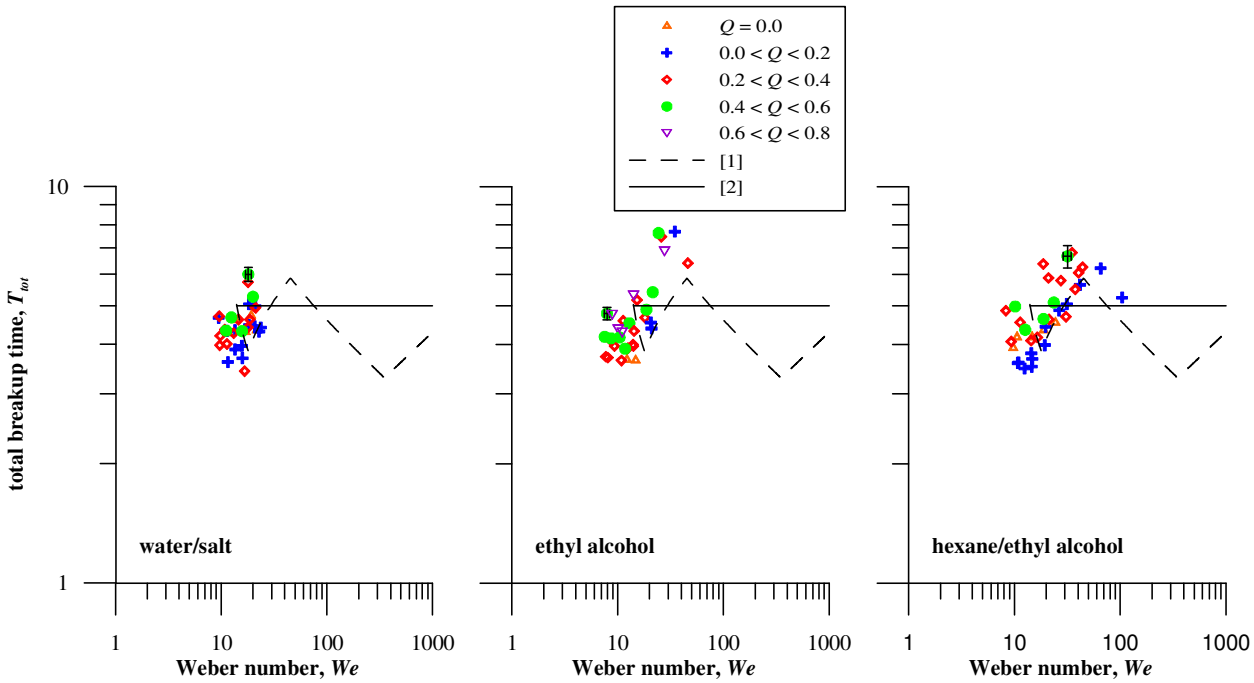


**Figure 6.** Charged Newtonian total breakup time, $T_{tot}$ (typical uncertainty bars shown)

Figure 6 shows $T_{tot}$ as a function of *We*. The number of data points is smaller because, in many cases, the drop left the camera field of view before breakup was complete. $T_{tot}$ could not be determined in those cases. Again, the data are compared to previous results for *uncharged* drops [1, 2]. Scatter in our $T_{tot}$ data is comparable to scatter in previous investigations of *uncharged* drops [1]. Most of it can be attributed to difficulty in determining the exact moment when breakup ceases.

Figure 5 and Figure 6 data indicate that charge has no discernable impact on $T_{ini}$ or $T_{tot}$.

## Conclusions

Despite the presence of electrostatic stresses, the addition of charge has a minimal effect on secondary atomization. This can be understood by considering how the charge distribution evolves as the drop deforms.

The first phase of drop breakup is deformation of the initially spherical drop into a shape that can be approximated as an oblate spheroid [4]. This increases the total surface area of the drop. Because charge is conserved, the mean surface charge density decreases, and by Eq. (3) the mean electrostatic stress also decreases.

However, as the drop deforms, electric and fluid dynamic effects result in a surface charge density that is a function of position and time. Therefore, while the *mean* electrostatic stress decreases, the *local* electrostatic stress may increase on some portion of the deformed drop. Furthermore, deformation results in non-constant surface curvature. Therefore, the restorative surface tension stress is also a function of position.

A complete analysis must compare the restorative surface tension stresses and disruptive electrostatic stresses over the entire surface of the deformed drop. In general the problem is governed by Maxwell's equations for the electric field coupled with the Navier-Stokes equations of fluid dynamics, and numerical solution is required. Here we take an alternative approach and consider limiting cases where analytic solutions can be derived.

When $K \ll T_{tot}$ the drop is nearly a perfect conductor. In that case, a closed form solution for $\gamma$ on an oblate spheroid is available in [18]. From this, the electrostatic stress as a function of position on the deformed drop, $\Delta p_{e^-}$, can be calculated using Eq. (3). Furthermore, the stress due to surface tension, $\Delta p_\sigma$, can be derived from an expression for surface curvature [19]. Combining these reveals that the *maximum* value of $\Delta p_{e^-}/\Delta p_\sigma$ is [19]:

$$\left(\Delta p_{e^-}/\Delta p_\sigma\right)_{\max} = Q \qquad \text{(conductive drop)} \tag{10}$$

This occurs on the leading and trailing faces of the flattened drop where surface curvature, and hence stress due to surface tension, is minimum.

This analysis also reveals that the ratio of electrostatic stress to surface tension stress never exceeds its initial value, $Q$. Therefore, the effective electrostatic stresses are decreasing (or constant) on the surface of a deforming conductive drop. Consequently, charge has a minimal effect on the secondary atomization.

The second liming case occurs when $K>>T_{tot}$. In this case, the drop is non-conductive and can support an internal electric field. Eq. (3) is no longer valid, and the more general expression given in [20] is required. Furthermore, assuming that the drop is a linear isotropic dielectric with a known $\gamma$, an analytic solution of the electric field can be found from a series solution of the electrostatic potential. [19] contains the full derivation and the final equations.

For the non-conductor, the charge distribution is coupled to the fluid motion. A solution of the governing equations requires significant computational effort and has not been attempted. Rather, $\gamma$ is assumed uniform over the drop surface. While this assumption is likely unrealistic, it is theorized to be a worst case scenario for which the drop is least stable.

Figure 7 shows the maximum ratio of electrostatic to surface tension stress for the case of a non-conductive drop with a uniform charge distribution. $d_{cro}$ is the cross-stream diameter of the deformed drop and $d_{str}$ is the stream-wise diameter as shown in Figure 1. Due to the simplifying assumptions discussed above, only qualitative conclusions can be made.

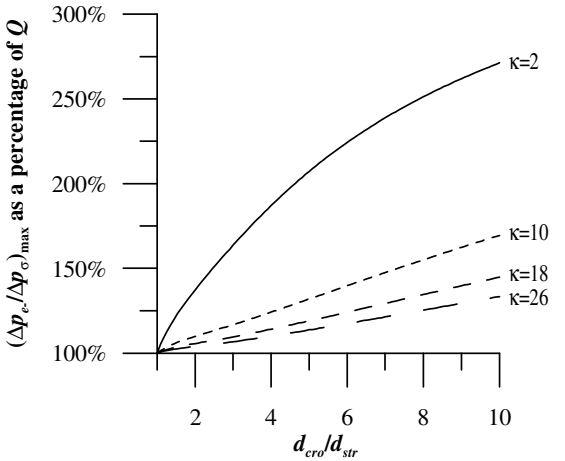


**Figure 7.** Maximum ratio of electrostatic to surface tension stress for a non-conductive drop versus deformation

In general the analysis predicts an increase in the effective electrostatic stresses over some portions of the drop during deformation. This is opposite to the case of the conductive drop and may explain the slight reduction in the stability for $K>0.01$ at low $We$. Regardless of conductivity, at high $We$ aerodynamic forces dominate the breakup and no effect of charge is observed.

Finally, in our previous work, [10, 11], a limited amount of data led us to conclude that $We_{e^-}$ can be used to correlate breakup of charged drops. Having significantly expanded the data set, we now argue that this is not the general case. Rather, breakup of charged drops appears to be governed by the phenomena discussed here.

**References**

[1] Pilch, M., and Erdman, C. A., *Int J Multiphase Flow* 13(6): 741-757 (1987).
[2] Hsiang, L. P., and Faeth, G. M., *Int J Multiphase Flow* 18(5): 635-652 (1992).
[3] Gelfand, B. E., *Prog Energy Combust Sci* 22(3): 201-265 (1996).
[4] Guildenbecher, D., López-Rivera, C., and Sojka, P., *Experiments in Fluids* 46(3): 371-402 (2009).
[5] Ranger, A. A., and Nicholls, J. A., *AIAA Journal* 7(2): 285-290 (1969).
[6] Griffiths, D. J., *Introduction to Electrodynamics*, Prentice Hall (1989).
[7] Rayleigh, L., *Philosophical Magazine* 14: 184-186 (1882).
[8] Shrimpton, J. S., and Laoonual, Y., *Int J for Numerical Methods in Engineering* 67: 1063-1081 (2006).
[9] Cloupeau, M., and Prunet-Foch, B., *J of Electrostatics* 25: 165-184 (1990).
[10] Guildenbecher, D., and Sojka, P., *ASME International Mechanical Engineering Congress and Exposition*, Seattle, Washington, (2007).
[11] Guildenbecher, D., and Sojka, P., *22nd European Conference on Liquid Atomization and Spray Systems*, Como Lake, Italy, (2008).
[12] Uematsu, M., and Frank, E. U., *J of Physical Chemistry Reference Data* 9(4): 1291-1306 (1980).
[13] Riddick, J. A., and Bunger, W. B., *Organic Solvents, Physical Properties and Methods of Purification*, Wiley-Interscience (1970).
[14] Zdanowski, M., Wolny, S., Zmarly, D. O., and Boczar, T., *J of Electrostatics* 65(4): 239-243 (2007).
[15] Klein, S., and Mcclintock, F., *Mechanical Engineering* 75: 3-8 (1953).
[16] Gamero-Castañoa, M., and Hruby, V., *J of Fluid Mechanics* 459: 245-276 (2002).
[17] Lee, C. H., and Reitz, R. D., *Int J Multiphase Flow* 26(2): 229-244 (2000).
[18] Stratton, J. A., *Electromagnetic Theory*, McGraw-Hill (1941).
[19] Guildenbecher, D. R., *Secondary Atomization of Electrostatically Charged Drops*, PhD Thesis, Purdue University (2009).
[20] Melcher, J. R., *Continuum Electromechanics*, The MIT Press (1981).